Striatal cholinergic interneurons generate beta and gamma oscillations in the corticostriatal circuit and produce motor deficits

Krishnakanth Kondabolu[a,1], Erik A. Roberts[a,1], Mark Bucklin[a], Michelle M. McCarthy[b], Nancy Kopell[b,2], and Xue Han[a,2]

[a]Department of Biomedical Engineering, Boston University, Boston, MA 02215 and [b]Department of Mathematics, Boston University, Boston, MA 02215

Contributed by Nancy Kopell, April 16, 2016 (sent for review December 28, 2015; reviewed by John T. Gale, Yanhua Huang, and Gavin L. Woodhall)

Cortico-basal ganglia-thalamic (CBT) neural circuits are critical modulators of cognitive and motor function. When compromised, these circuits contribute to neurological and psychiatric disorders, such as Parkinson's disease (PD). In PD, motor deficits correlate with the emergence of exaggerated beta frequency (15–30 Hz) oscillations throughout the CBT network. However, little is known about how specific cell types within individual CBT brain regions support the generation, propagation, and interaction of oscillatory dynamics throughout the CBT circuit or how specific oscillatory dynamics are related to motor function. Here, we investigated the role of striatal cholinergic interneurons (SChIs) in generating beta and gamma oscillations in cortical-striatal circuits and in influencing movement behavior. We found that selective stimulation of SChIs via optogenetics in normal mice robustly and reversibly amplified beta and gamma oscillations that are supported by distinct mechanisms within striatal-cortical circuits. Whereas beta oscillations are supported robustly in the striatum and all layers of primary motor cortex (M1) through a muscarinic-receptor mediated mechanism, gamma oscillations are largely restricted to the striatum and the deeper layers of M1. Finally, SChI activation led to parkinsonian-like motor deficits in otherwise normal mice. These results highlight the important role of striatal cholinergic interneurons in supporting oscillations in the CBT network that are closely related to movement and parkinsonian motor symptoms.

striatum | optogenetics | beta oscillations | coherence | cholinergic interneurons

Exaggerated beta oscillations (15–30 Hz) within the cortico-basal ganglia-thalamic (CBT) neural network are putative electrophysiological correlates of bradykinesia and rigidity in Parkinson's disease (PD) (1–4). Therapies that effectively manage PD motor symptoms, such as dopamine replacement therapy and deep brain stimulation, are associated with a suppression of the exaggerated beta oscillations (4, 5). Beta oscillations are also found in the CBT circuits of patients with other movement-related disorders, such as epilepsy and dystonia (6, 7), and in normal, nonhuman primates (8, 9) and normal rodents (10, 11). Moreover, brief elevations (≤200 ms) of beta oscillations are observed in the basal ganglia of task-performing nonhuman primates and rodents during specific phases of behavioral tasks (10, 12, 13), indicating that beta oscillations may be important for motor and nonmotor functions. In contrast to the regulated temporal variability of beta oscillations in normal motor functions, temporal stability is correlated with the parkinsonian motor symptoms of bradykinesia and rigidity (2). Together, these findings suggest that brief epochs of beta oscillations are a normal aspect of basal ganglia dynamics, their temporal modulation is important for movement regulation, and loss of regulation or uncontrolled expression of beta oscillations may contribute to movement deficits, such as those observed in PD.

Despite the clear link between CBT beta oscillations and movement, the mechanisms underlying their generation remain elusive. Dopamine clearly modulates the generative mechanisms of CBT beta oscillations and beta frequency coherence between CBT structures. A hallmark of PD pathology is chronic reduction of dopamine input to CBT circuits due to midbrain dopaminergic neuron loss. Loss of midbrain dopamine increases beta oscillation power and coherence in PD animal models (14, 15). Similarly, acute reduction of dopamine locally in the striatum increases striatal beta oscillations (16). Systemic dopaminergic drugs decrease beta oscillation power and coherence in PD patients (17), and also increase finely tuned gamma oscillations in the basal ganglia and thalamus, although we know little about the functional significance of these finely tuned gamma oscillations in PD (17, 18). Because of the dense innervation of the striatum by the midbrain dopaminergic system (19), we have recently proposed that dopamine may modulate basal ganglia beta oscillations by acting on the striatum, in particular via the striatal cholinergic system. Dopamine, acting on D2 receptors, provides tonic suppression of acetylcholine (ACh) release in the striatum (20). Under conditions of low striatal dopaminergic tone, such as in PD, increased cholinergic tone may play a more prominent role in modulating striatal dynamics, such as supporting the generation of exaggerated beta oscillations (21–23). Additionally, the striatum contains high levels of cholinergic markers (24), highlighting a prominent role for cholinergic regulation in striatal function.

Recently, we demonstrated that direct local infusion of the cholinergic agonist carbachol into the striatum of normal mice can generate robust beta oscillations within the striatum (23). Using computational approaches, our previous study predicted that increased striatal cholinergic tone could lead to elevated beta oscillations through activation of muscarinic receptors that lead to the suppression of M current in the striatal medium spiny neurons. Here, to further demonstrate the function of the

Significance

Exaggerated beta oscillations within the cortico-basal ganglia-thalamic (CBT) network are putative electrophysiological signatures of bradykinesia and rigidity in Parkinson's disease (PD). However, it is unclear how exaggerated beta oscillations emerge and how such oscillation patterns are related to PD motor deficits. In this study, we demonstrate that a single cell type, the striatal cholinergic interneuron, mediates the emergence of exaggerated beta oscillations within CBT circuits of normal mice and induces parkinsonian-like motor deficits. Because the striatal cholinergic system is uninhibited by loss of dopamine, these results provide mechanistic insights into the therapeutic effects of anticholinergic drugs in the treatment of PD and highlight the potential for developing beta oscillation-based biomakers for PD.

Author contributions: K.K., E.A.R., M.M.M., N.K., and X.H. designed research; K.K., E.A.R., M.M.M., and X.H. performed research; K.K., E.A.R., M.B., M.M.M., N.K., and X.H. contributed new reagents/analytic tools; K.K., E.A.R., M.B., M.M.M., and X.H. analyzed data; K.K., E.A.R., M.M.M., N.K., and X.H. wrote the paper; and N.K. and X.H. supervised the study.

Reviewers: J.T.G., Cleveland Clinic; Y.H., University of Pittsburgh; and G.L.W., Aston University.

The authors declare no conflict of interest.

[1]K.K. and E.A.R. contributed equally to this work.

[2]To whom correspondence may be addressed. Email: xuehan@bu.edu or nk@bu.edu.

This article contains supporting information online at www.pnas.org/lookup/suppl/doi:10.1073/pnas.1605658113/-/DCSupplemental.

intrinsic striatal cholinergic system in modulating neural dynamics of the CBT network and the related receptor mechanisms, we selectively activated striatal cholinergic interneurons (SChIs) by using optogenetic techniques, while simultaneously recording local field potentials (LFPs) in the striatum and the primary motor cortex (M1), with or without local infusion of selective cholinergic receptor antagonist. We found that brief optogenetic stimulation of SChIs acutely elevated beta oscillations in the striatum and all cortical layers of M1, and gamma oscillations in the striatum and deeper layers of M1. Increased oscillations were accompanied by increased coherence between striatum and M1 in a layer-dependent manner. In addition, local striatal infusion of the muscarinic receptor blocker scopolamine, but not the nicotinic receptor blocker mecamylamine, reduced striatal beta oscillations. Finally, we assessed the effect of SChI stimulation on locomotion and found that activation of SChIs decreased movement, increased immobility, and increased rotation. Together, these results demonstrate that activation of SChIs can generate elevated beta and gamma oscillations and coherence in the cortico-striatal network in a cortical layer-dependent manner via muscarinic receptors, and alter locomotion behavior.

Methods Summary

Technical details are in *SI Methods Summary*. Briefly, all animal procedures were approved by the Boston University Institutional Animal Care and Use Committee (IACUC). Surgically implanted adult mice were recorded awake, head-fixed. Recordings were made simultaneously in the striatum [stereotactic coordinates 0 anterior-posterior (AP), 2.5–3 medial-lateral (ML), 2–2.5 depth] by using a glass pipette to avoid photoelectric effects during optogenetic laser illumination, and in the primary motor cortex (M1) by using laminar electrodes containing 16 electrode contacts spaced at 100 μm, positioned across the entire cortical depth (coordinates 1.5–2 AP, 1.25–1.5 ML). To optogenetically activate SChIs, a fiber was coupled to a 473-nm laser. All data analysis was performed in MATLAB. Statistics were performed in MATLAB or GraphPad Prism.

Results

Selective Optogenetic Activation of SChIs Increased Striatal Alpha, Beta, and Gamma Oscillations. We recently demonstrated that the striatal cholinergic system can support the generation of beta oscillations by using a combination of mathematical modeling and experimental techniques that combined in vivo electrophysiology with local infusion of the nonselective cholinergic agonist carbachol (23). To further explore the ability of intrinsic SChIs in modulating beta oscillations throughout the CBT network, we recorded LFPs in the striatum and the primary motor cortex (M1), while optogenetically activating SChIs in transgenic choline acetyltransferase promoter (Chat)-Channelrhodopsin-2 (ChR2) mice (Fig. 1*A*). Chat-ChR2 mice were generated by crossing Chat-Cre mice with Cre-regulated ChR2-reporter mice (Ai32), resulting in selective ChR2 expression in Chat-positive SChIs (Fig. 1*B*). Control groups consisted of Ai32 transgenic littermates that did not express ChR2 protein because of the lack of Cre recombinase expression, despite the presence of ChR2 genes in the genome. An optical fiber coupled to a glass electrode was positioned in the dorsal striatum for simultaneous optogenetic stimulation and LFP recordings. Glass electrodes were used to record LFPs at the site of laser illumination to avoid photoelectric effects that are routinely observed on electrodes made of other materials (Fig. 1*A*) (25).

Optogenetic activation of SChIs with a Poisson-distributed 40-Hz laser light pulse train robustly increased oscillations across broad frequencies in the striatum (Fig. 2 *C* and *D*). The increase in oscillation power persisted for several hundred milliseconds after laser offset (Fig. 2 *C* and *D*), suggesting that direct patterning of SChIs by laser pulses was unlikely to account for the elevated oscillations at these frequencies. To further evaluate the changes at specific frequency bands, we calculated the normalized spectrum before, during, and after laser stimulation. We found that optogenetic stimulation of SChIs robustly increased oscillation power across higher frequency bands conventionally defined as alpha (8–15 Hz), beta (15–30 Hz), low gamma (30–60 Hz), and high gamma (60–100 Hz), but not lower frequency bands of delta (1–4 Hz) or theta (4–8 Hz) (Fig. 2 *E* and *F*; $n = 7$ mice). A similar laser illumination protocol in Ai32 control mice failed to alter oscillation power at any frequency ($n = 5$ mice, $P > 0.05$ for all bands, signed-rank test), confirming that the observed changes in Chat-ChR2 mice are due to optogenetic activation of SChIs.

To further rule out the possibility that the observed oscillation changes were due to direct activation of SChIs, we tested a set of seven additional laser illumination parameters, including 5-s-long constant laser illumination, 1-s-long fixed interval pulse trains at 50 and 100 Hz, as well as Poisson-distributed pulse trains at 4, 9, 20, and 40 Hz. Because of the large LFP deflections induced by optogenetic stimulation of SChIs during the 1-s stimulation, it was difficult to reliably estimate the power changes during laser stimulation. Thus, we analyzed the 1-s period immediately following laser offset. In general, we observed similar increases in beta and gamma oscillations by using these stimulation patterns (Figs. S1*B* and S2; $n = 5$ mice, $P \leq 0.05$, signed-rank test). Together, these results demonstrate that direct activation of SChIs generates robust beta and gamma oscillations within the striatum that are independent of the particular optogenetic stimulation pattern and persist for an extended period after the offset of light illumination, suggesting that these oscillations emerge from dynamic network interactions upon an increase in the striatal cholinergic tone.

SChI Activation Leads to Layer-Dependent Beta and Gamma Oscillation Changes in the M1. To understand the influence of the oscillations induced by optogenetic stimulation of SChIs on the rest of the CBT network, we performed simultaneous recordings in M1 by using a laminar electrode containing 16 contacts spaced at 100 μm, which can identify cortical layer-dependent changes (Fig. 3 *A* and *B*). We did not observe laser-induced photoelectric artifacts on the laminar electrodes in M1. Because they were ~2 mm away from the striatal

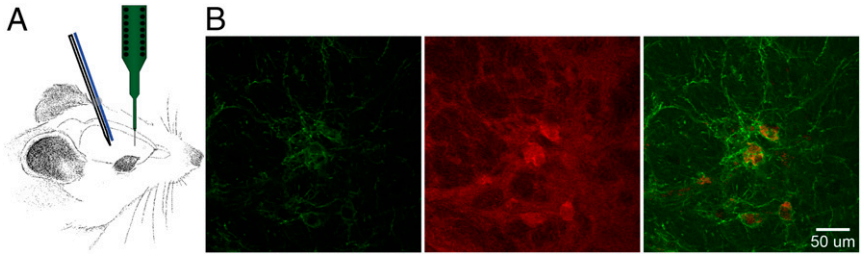

Fig. 1. Experimental setup and protocols. (*A*) Illustration of the recording configuration. The recording pipette was coupled to an optical fiber and a laminar probe containing 16 electrode contacts, positioned in the M1. (*B*) A representative image of the striatum showing ChR2-eYFP fluorescence (green; *Left*), immunofluorescence of ChAT (red; *Middle*), and colocalization (*Right*).

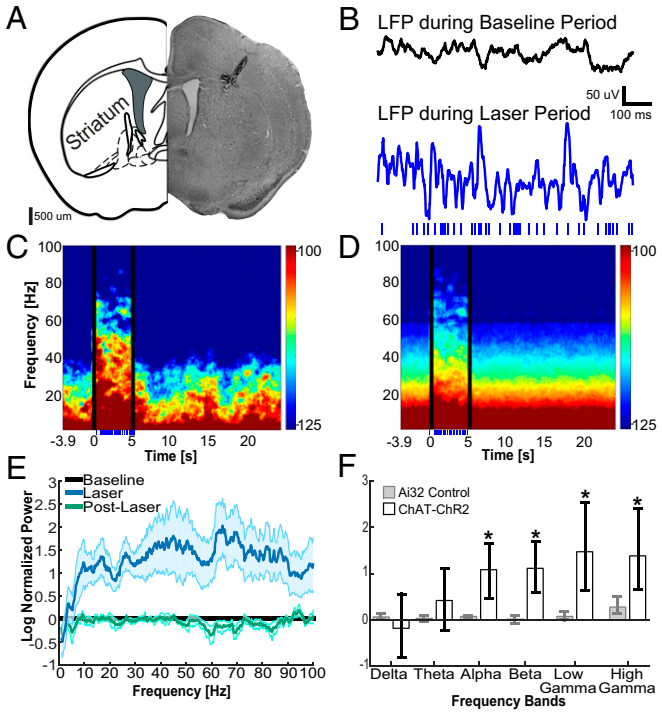

Fig. 2. Optogenetic activation of SChIs increased striatal alpha, beta, and gamma oscillations. (*A*) Representative coronal histological section showing an electrode and optical fiber track into the striatum. (*B*) Representative 1-s LFPs recorded in the striatum before (*Top*) and during (*Bottom*) laser stimulation at Poisson-distributed 40 Hz (*Bottom*; blue dashes indicate the time of laser pulses). (*C*) Representative spectrogram from one mouse, aligned to laser onset and averaged over all trials. The 500 ms immediately after laser onset and offset were excluded from the corresponding statistics because of strong LFP deflections. (*D*) Population spectrogram upon optogenetic stimulation of SChIs in ChAT-ChR2 mice ($n = 7$ mice). (*E*) Population power spectrum normalized to baseline, across frequencies before (Baseline, black), during (blue), and after laser stimulation (green), in the Chat-ChR2 mice ($n = 7$ mice). The shaded area around each solid line represents the SEM. (*F*) Bar plots comparing changes upon laser stimulation in different frequency bands between the Chat-ChR2 experimental group and the Ai32 control group for delta (1–4 Hz), theta (4–8 Hz), alpha (8–15 Hz), beta (15–30 Hz), low gamma (30–60 Hz), and high gamma (60–100 Hz) oscillations. The error bars represent the bootstrapped 95% confidence intervals (*$P \leq 0.05$, nonparametric signed-rank test).

laser illumination site, <0.1% of laser light was expected to reach M1 (25). Optogenetic activation of SChIs in the striatum coincided with robust LFP voltage deflections across all cortical depths in M1 (Fig. 3*B*), and oscillation power consistently increased with cortical depth (Fig. 3*C*). To compare the difference in LFPs across anatomically defined cortical layers, we averaged the power spectra recorded at different depths, with the first 500 μm corresponding to the superficial layers, 500–800 μm corresponding to the middle layers, and 900–1,200 μm corresponding to the deep layers.

Beta frequency power consistently increased in all M1 layers during SChI stimulation. In contrast, gamma frequency power, both high gamma and low gamma, were selectively increased in the deep layers, but not the superficial layers (Fig. 3 *D*–*F*). In the middle layers, high gamma power was elevated, but not low gamma power. We observed small but nonsignificant changes in delta, theta, and alpha frequencies across all layers. Together, these results provide direct evidence that SChI activation can enhance beta oscillations in all M1 layers, and gamma oscillations in a cortical layer-dependent manner. These SChI activation-induced beta and gamma oscillations across different M1 layers suggest that beta oscillations can be widely expressed by neuronal ensembles within different M1 cortical layers, whereas gamma oscillations are selectively expressed in deeper layers, although it is unknown how different cell types within each M1 layer uniquely support these oscillations.

SChI Activation Modulates Coherence Between the Striatum and M1. To evaluate the synchronization of oscillations between the striatum and M1 upon optogenetic activation of SChIs, we calculated the coherence of the LFPs recorded in these two structures before and during laser stimulation. We found an increase in coherence during laser stimulation between deep layers of M1 and the striatum at both beta and low gamma frequencies, but not at high gamma frequencies (Fig. 4; $P \leq 0.05$, jackknife test). This increased coherence is consistent with the idea that deep M1 layers contribute to M1-striatal coordination through direct axonal projections. However, we note that although the coherence at beta frequencies below 23 Hz is maintained throughout the simulation, coherence at higher beta frequencies dissipates rapidly after the first second of stimulation, suggestive of multiple independent beta oscillations within the 15–30 Hz range defined here.

The lack of coherence changes at high gamma frequencies suggests that the observed increase in high gamma power may be due to increased local neuronal activity within M1 (26). In the middle layer, where both beta and high gamma power increased, we observed a significant increase in coherence at beta frequency, but not at high gamma frequencies (Fig. 4). Considering that middle layers of M1 do not directly connect to the striatum, the observed increase in coherence at beta frequencies are likely coordinated or relayed through other structures, such as the thalamus that directly project to the middle layer, especially layer 4. Surprisingly, despite the increase in superficial layer beta power, activation of SChIs resulted in significant attenuation of coherence at beta and gamma frequencies (Fig. 4; $P \leq 0.05$, jackknife test), suggesting that oscillations within the striatum and superficial M1 are independently regulated. In summary, activation of SChIs in the striatum appears to engage multiple independent beta generators that interact in the CBT network in a cortical layer-dependent manner, whereas high gamma oscillations are locally generated.

Striatal Muscarinic Receptors Mediate SChI-Induced Beta and Low Gamma Oscillations in the Corticostriatal Network. To understand the receptor mechanism by which SChIs engage the striatum and M1 to generate beta and gamma oscillations, we combined optogenetic activation of SChIs with local intracranial infusion of selective cholinergic receptor antagonists. We infused either the muscarinic antagonist scopolamine (100 μg/μL) or the nicotinic antagonist mecamylamine (10 μg/μL) into the striatum, and optogenetically activated SChIs while simultaneously recording LFPs in the striatum and M1.

We observed that scopolamine infusion in the striatum broadly decreased oscillation power in the striatum across all frequencies analyzed (approximately from 2 to 100 Hz, Fig. 5*A*; $n = 8$ mice; >2 SEM). A similar reduction in oscillation power was also observed in the middle and deep layers of M1, although not at very low frequencies of ∼2–5 Hz, (Fig. 5*B*; $n = 8$ mice). Interestingly, no change in power was observed in the superficial layers of M1, suggesting that oscillatory dynamics in the superficial layers are only loosely coupled to the CBT network (Fig. 5 *B*, *i*). Together these results demonstrate that intrinsic striatal muscarinic tone is responsible for basal levels of oscillations across broad frequencies in the striatum and deeper layers of M1.

We next tested the effectiveness of optogenetic activation of SChIs in generating oscillations in the presence of muscarinic or nicotinic receptor blockers. Because of the reduction of oscillation power across all frequencies upon scopolamine infusion, we cannot directly compare the effects of optogenetic stimulation in the presence of scopolamine to that observed in the absence of scopolamine. We thus compared the effect of optogenetic activation of SChIs in the presence of scopolamine and found that

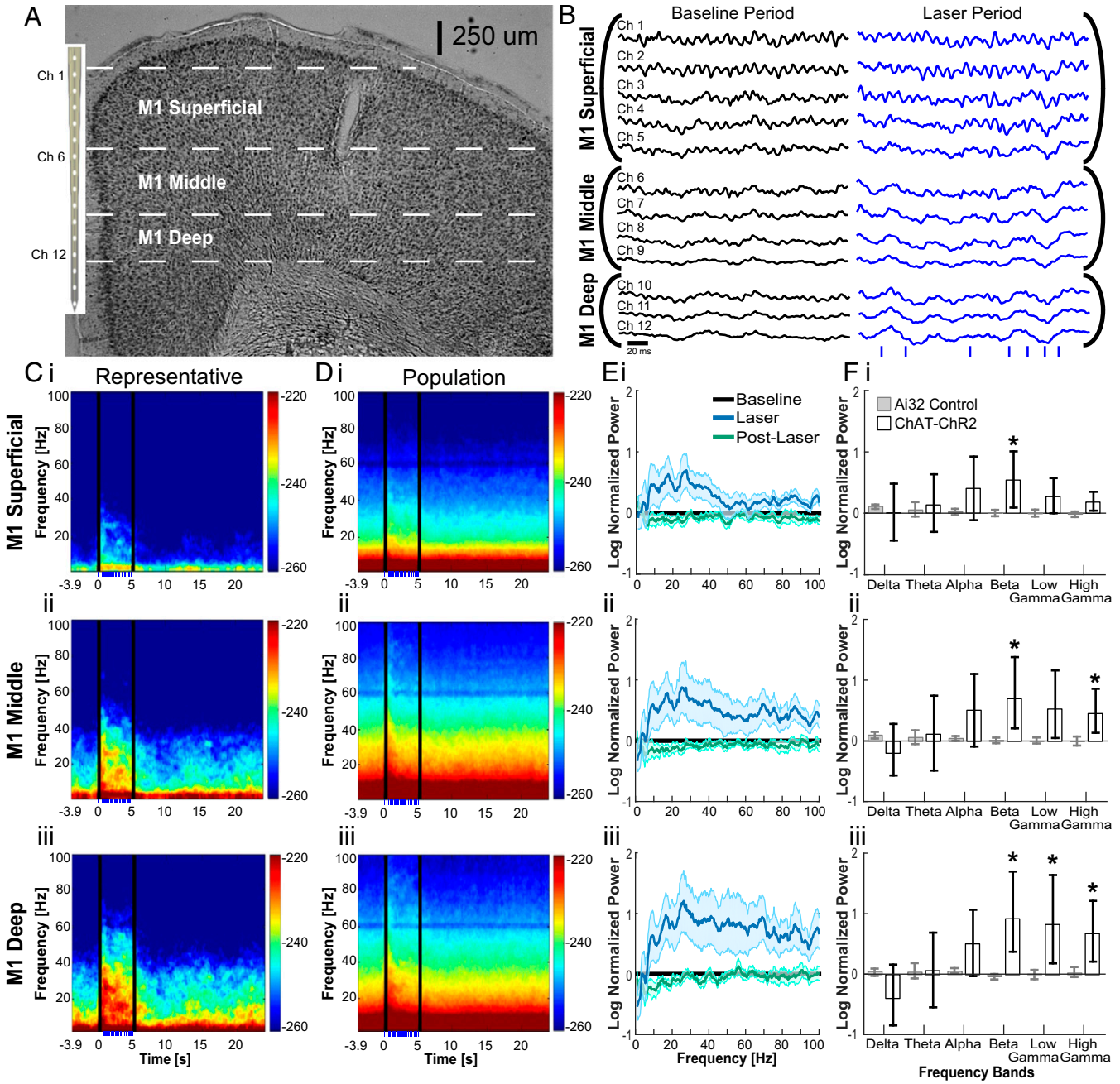

Fig. 3. SChI activation led to layer-dependent beta and gamma oscillation changes in the M1. (*A*) Representative coronal section demonstrating the position of laminar electrodes in M1. (*B*) Representative 200-ms LFPs during the baseline period before laser simulation (black) and during laser stimulation period (blue). (*C*) Representative power spectrum from an individual mouse for superficial layers (*C*, *i*, averaged across Ch1–Ch5), middle layers (*C*, *ii*, averaged across Ch6–Ch9), and deep layers (*C*, *iii*, averaged across Ch10–Ch12). The 500 ms immediately after laser onset and offset were excluded from the corresponding statistics because of strong LFP deflections. (*D*) Population spectrograms aligned to laser onset for superficial layers (*D*, *i*), middle layers (*D*, *ii*), and deep layers (*D*, *iii*) ($n = 7$ mice). Bottom, blue dashes indicate the timing of laser light pulsed at Poisson-distributed 40 Hz, for 5 s. (*E*) Population spectrum for M1 superficial layers (*E*, *i*), middle layers (*E*, *ii*), and deep layers (*E*, *iii*). (*F*) Bar plots comparing oscillation powers at different frequencies in superficial (*F*, *i*), middle (*F*, *ii*), and deep (*F*, *iii*) layers for delta (1–4 Hz), theta (4–8 Hz), alpha (8–15 Hz), beta (15–30 Hz), low gamma (30–60 Hz), and high gamma (60–100 Hz). Error bars represent the bootstrapped 95% confidence intervals (*$P \leq 0.05$, nonparametric signed-rank test).

activation of SChIs in the presence of the muscarinic blocker scopolamine remained effective at inducing beta, low gamma, and high gamma oscillations in the striatum (Fig. 6 *B*, *i* and *C*, *i*; $P \leq 0.05$, bootstrap test). However, the increases were relatively weaker compared with that observed without scopolamine (Fig. 6 *A*, *i*). In M1, SChI stimulation in the presence of scopolamine failed to alter beta, low gamma, or high gamma power from the prestimulation baseline in any cortical layer (Fig. 6 *B*, *ii–iv* and *C*, *ii–iv*; $P > 0.05$, signed-rank test). Infusion of artificial cerebrospinal fluid (ACSF) or the nicotinic antagonist mecamylamine failed to alter oscillation power at any frequency in the striatum or M1, compared with the preinfusion baseline (Fig. 5) (Fig. S3, $n = 6$ mice infused with mecamylamine; and Fig. S4, n = 5 mice infused with ACSF; $P > 0.05$, signed-rank test). Together, these results

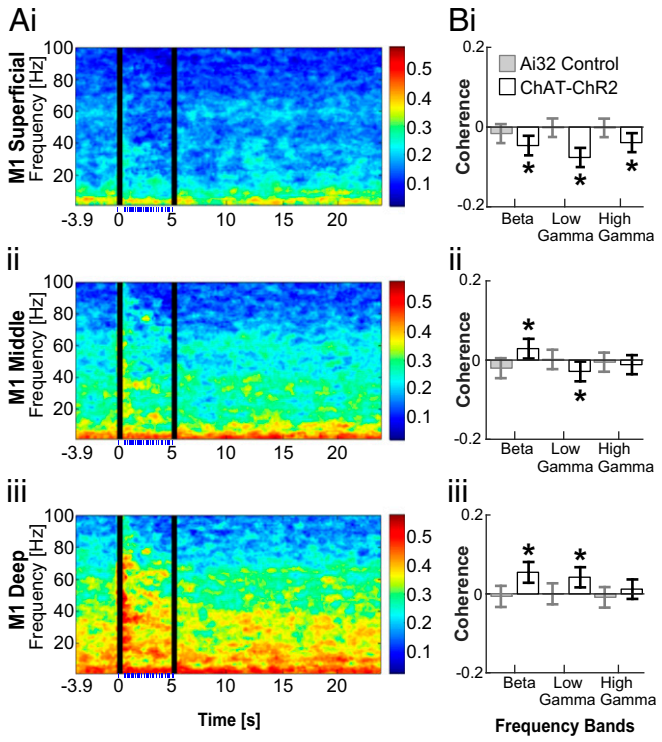

Fig. 4. SChI activation modulated coherence between the striatum and M1. (*A*) Population coherograms show coherence between the striatum and superficial (*i*), middle (*ii*), and deep layers (*iii*) of M1 before, during, and after laser stimulation. Laser stimulation was pulsed at a Poisson-distributed 40 Hz, during 0–5 s (bottom, blue dashes indicate the timing of laser pulses, $n = 7$ mice). The 500 ms immediately after laser onset and offset were excluded from the corresponding statistics because of strong LFP deflections. (*B*) Bar plots comparing the coherence between the striatum and M1 superficial (*B, i*), middle (*B, ii*), and deep (*B, iii*) layers before and during laser stimulation for beta (15–30 Hz), low gamma (30–60 Hz), and high gamma (60–100 Hz) frequencies. Error bars indicate the jackknifed 95% confidence interval error bars (*$P \leq 0.05$, nonparametric jackknife test).

suggest that cholinergically induced elevation of beta and gamma oscillations in the striatum is mediated by striatal muscarinic receptors, but not by striatal nicotinic receptors. The fact that in the presence of scopolamine, SChI activation only elevated striatal oscillations, but not M1 oscillations, suggests that striatal beta oscillations are independent of phasic beta input from M1, supporting the existence of a basal ganglia generator of beta oscillations. These results further suggest that the elevation in M1 beta oscillations depends on active muscarinic mechanisms in the striatum.

Unilateral SChI Activation Decreases Locomotion and Increases Rotation Behavior. To evaluate whether a transient increase in striatal cholinergic tone is sufficient to alter locomotion, we optogenetically stimulated SChIs in another group of freely moving mice. To optimize the illumination volume, we designed a fiber array containing four optical fibers unilaterally targeting a large fraction of the dorsolateral striatum that receives M1 inputs (27) in Chat-ChR2 mice ($n = 5$ mice), or control Ai32 mice ($n = 5$ mice). We monitored the locomotion in a custom arena while optogenetically stimulating SChIs by using the same light illumination pattern at Poisson-distributed 40 Hz, but illuminated for 2 min to better quantify behavioral effects (Fig. 7*A*). Locomotion was monitored for 8 min/d, over 7 consecutive days.

We first estimated the overall effect of stimulating SChIs on locomotion by calculating the total distance traveled during each 2-min period before, during, and after laser illumination and found that optogenetic activation of SChIs significantly reduced the total distance traveled compared with the pre-laser baseline period (Fig. 7 *B* and *C*; $P \leq 0.001$, Bonferroni-corrected nonparametric paired signed-rank tests). This reduction persisted for an additional 2 min immediately after laser offset (post-laser 1) ($P \leq 0.001$, paired signed-rank test) and returned to baseline in the subsequent 2-min interval (Post-Laser 2) ($P > 0.05$, paired signed-rank test). Further analysis indicated that locomotion reduction resulted from increased immobility, defined as the percentage of time when movement was smaller than 1.5 cm/s (Fig. 7*D*; $P \leq 0.001$, paired signed-rank test), as well as decreased movement speed (Fig. 7*E*; $P \leq 0.001$, paired signed-rank test). The same optogenetic analysis in control Ai32 mice did not produce any change in locomotion, immobility, or movement speed ($n = 5$, $P > 0.05$ for all periods analyzed, paired signed-rank test), confirming that the observed locomotion deficit was due to optogenetic activation of SChIs.

To further assess whether unilateral optogenetic stimulation of SChIs biases movement direction preference, we assessed rotation behavior. Interestingly, we found that stimulation of SChIs in one hemisphere resulted in a significant increase in both ipsilateral and contralateral rotations during the laser period (Fig. 7*F*; $P \leq 0.01$ and $P \leq 0.05$, respectively, paired signed-rank test). Similar analysis in control Ai32 mice did not yield any change in rotation behavior ($P > 0.05$, paired signed-rank tests). In the context of our experimental protocol, these results suggest that optogenetic activation of SChIs is not sufficient to bias movement direction preference in freely moving mice, but instead leads to an overall increase in rotation behavior. In summary, our results suggest that SChIs are critically involved in modulating locomotion, and that a selective increase in striatal cholinergic tone leads to direct motor behavioral deficits.

Discussion

We tested the role of intrinsic physiological striatal ACh release in modulating beta and gamma oscillations within cortico-striatal circuits. Combining optogenetics, pharmacology, electrophysiology, and behavioral assays in mice, we show that SChI activation reliably and reversibly increased alpha, beta, and gamma oscillations in the striatum. In M1, SChI stimulation increased beta power in all layers and gamma power in a layer-dependent manner. SChI-induced striatal and M1 beta and low gamma oscillations critically depended on striatal muscarinic receptors.

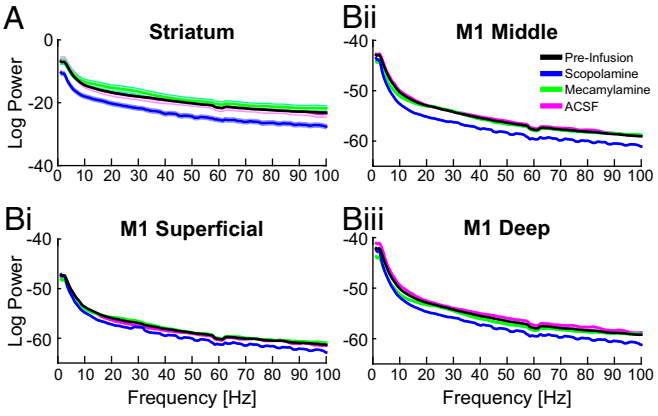

Fig. 5. Striatal muscarinic receptors modulated basal levels of beta and gamma oscillations in the striatum and deeper layers of M1. After striatal drug infusion, population power spectrums in the striatum (*A*), and different layers of M1 [superficial (*B, i*), middle (*B, ii*), and deep layers (*B, iii*)]. The shaded area around each solid line represents the SEM. Scopolamine infusion reduced oscillation power in the striatum, middle layers of M1, and deep layers of M1.

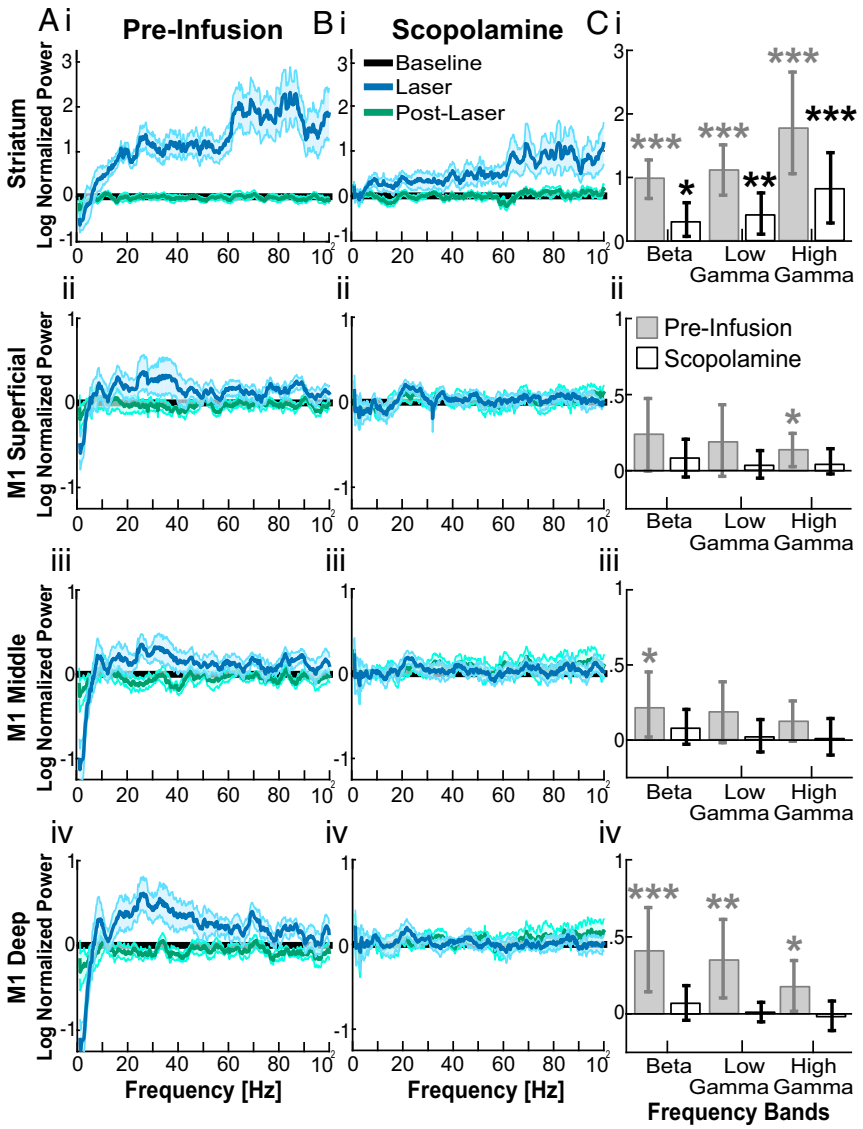

Fig. 6. Striatal muscarinic receptors mediated SChI-induced beta and gamma oscillations in the striatum and M1. (*A* and *B*) Optogenetic stimulation induced changes in the power spectrum before (*A*) and after (*B*) scopolamine infusion ($n = 8$ mice), in the striatum (*i*), superficial (*ii*), middle (*iii*), and deep layers of M1 (*iv*). The power spectrum during laser stimulation (blue) and after laser stimulation (green) was normalized to the baseline (black). (*C*) Bar plot comparison of oscillation power changes in beta (15–30 Hz), low gamma (30–60 Hz), and high gamma (60–100 Hz) frequencies, before (gray) and after (white) scopolamine infusion. Error bars are the bootstrapped 95% confidence intervals (*$P \leq 0.05$; **$P \leq 0.01$; ***$P \leq 0.001$; nonparametric bootstrap test).

Furthermore, SChI activation correlated with decreased locomotion and increased rotation behavior. Together, these results demonstrate that SChIs mediate changes in beta and gamma oscillations within the CBT circuit that are relevant to movement and movement deficits.

Activation of SChIs selectively increased higher frequency oscillations in the striatum, including alpha, beta, and gamma oscillations, but not lower frequency theta or delta oscillations. In our previous work, we found beta oscillations were elevated in striatum in response to the local infusion of the cholinergic agonist, carbachol (23). However, this study did not look at gamma oscillations and, thus, more work is needed to determine whether carbachol also elevates gamma frequency rhythms in striatum. In M1, SChI activation increased beta oscillations in all layers, and gamma oscillations only in middle and deep layers. Interestingly, despite the increase in beta, low gamma, and high gamma oscillations in the striatum and M1 deeper layers, the coherence between these two structures remained unchanged at high gamma frequencies during SChI activation, further confirming that these oscillations are supported by distinct mechanisms, with high gamma oscillations likely representing a local increase in neuronal excitability (26). Using conventionally defined frequency bands, we find SChI stimulation increased alpha oscillations (8–15 Hz) in striatum but not in M1. Interestingly, the PD motor symptoms of bradykinesia and rigidity are correlated with elevated beta oscillations in basal ganglia that can extend down to 8 Hz and, thus, includes the alpha frequency range (4, 28).

To determine the contributions of cholinergic receptor subtypes toward beta oscillation generation, we incorporated pharmacological techniques into our present study. Local infusion of scopolamine, a muscarinic receptor antagonist, in the striatum not only reduced oscillation powers across all frequencies analyzed, but also drastically reduced the evoked beta and gamma oscillations upon optogenetic stimulation of SChIs.

In contrast, scopolamine did not alter SChI-induced high gamma oscillations, suggesting a mechanistic separation between

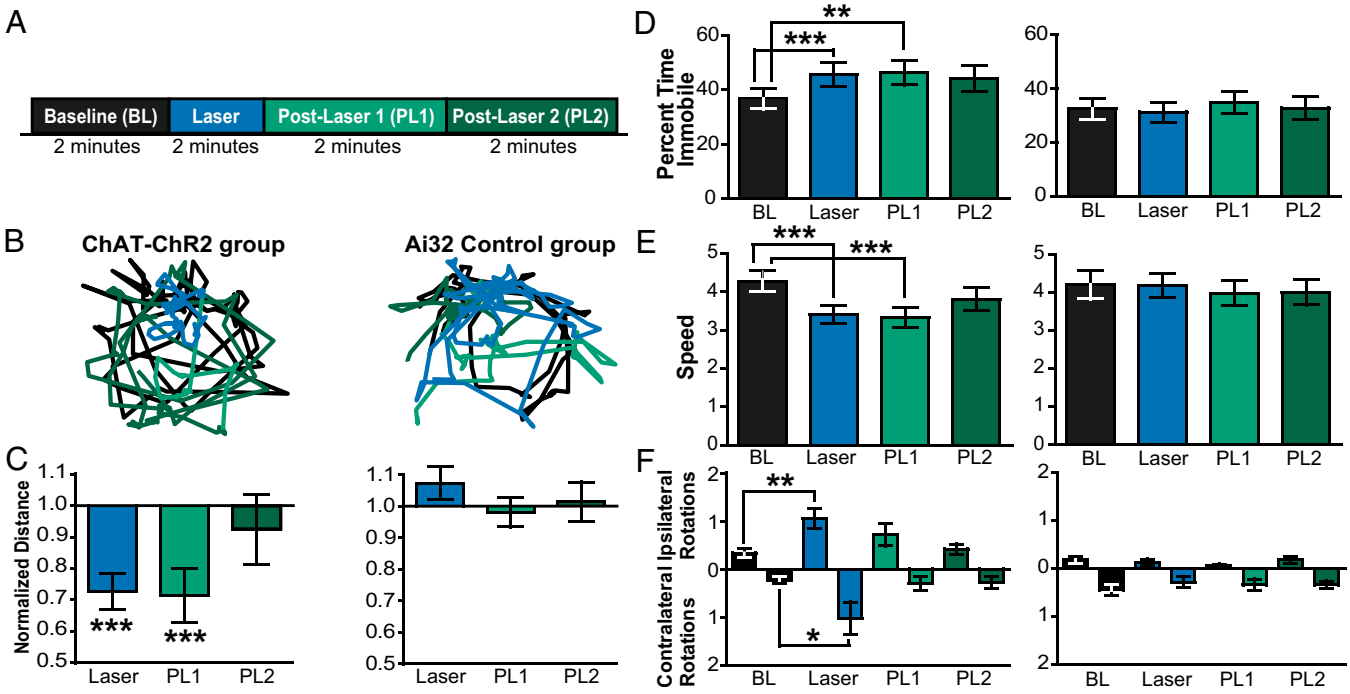

Fig. 7. Unilateral SChI activation decreased locomotion and increased rotation behavior. (*A*) Behavioral optogenetic experimental protocol consists of a baseline period, laser period, and two post-laser periods (2 min per period). (*B*) Representative positions of a ChAT-ChR2 mouse (*Left*) and a control Ai32 mouse (*Right*) before (black trace), during (blue trace), and post-laser periods (green traces) after laser illumination. (*C–E*) Bar plot comparison of locomotor activity measures, including baseline-normalized distance (C), percent time immobile (*D*), and movement speed when mobile (*E*). (*F*) Bar plot comparison of rotation in the Chat-ChR2 group (*Left*) and the control Ai32 group (*Right*) ($n = 5$ mice for Chat-ChR2 group; $n = 5$ mice for control Ai32 group). Error bars indicate the SEM (*$P \leq 0.05$; **$P \leq 0.01$; ***$P \leq 0.001$; Bonferroni-corrected nonparametric paired signed-rank tests).

the generators of beta/low gamma and high gamma oscillations. In contrast, the nicotinic receptor antagonist mecamylamine failed to change SChI-induced elevation of beta, low gamma, or high gamma oscillations in either the striatum or M1. These results demonstrate that SChIs exert rapid and powerful control over the dynamic generation of beta and gamma oscillations both within the striatum and throughout the CBT network through muscarinic mechanisms.

Beta frequency oscillations are found in the basal ganglia and the cortex of PD patients (29, 30) and PD animal models (15, 29, 31). Beta elevation correlates with the PD motor symptoms of bradykinesia and rigidity. The multiple plastic changes seen throughout the CBT loop due to chronic loss of dopamine are not present in our current experiments, and we do not consider the SChI stimulation state equivalent to the parkinsonian state. Indeed SChI stimulation-induced gamma oscillations and contralateral rotational behavior are not observed in parkinsonian states. Nevertheless, it is interesting that some parkinsonian phenomenology (elevated beta and hypokinetic movement) was evident during SChI stimulation despite normal dopaminergic function and lack of parkinsonian plastic changes. Interestingly, one recent study demonstrated that optogenetic inhibition of SChIs alleviated some parkinsonian motor symptoms in 6-hydroxydopamine (6-OHDA) mice (32). Together, these findings suggest that the CBT network components that modulate beta oscillations in normal states may be operational, but unmodulated, in PD states.

Striatal manipulations often produce alterations in behavior that generally can be classified as either hyperkinetic or hypokinetic. Examples of striatal perturbations resulting in hyperkinesia include inhibition of striatal fast spiking (FS) interneurons (33), optogenetic stimulation of D1 medium spiny neurons (MSNs) (34), and intrastriatal infusion of amphetamine (35). In contrast, hypokinetic movements are produced by optogenetic stimulation of striatal D2 MSNs (34). Here, we demonstrated that stimulation of SChIs also resulted in hypokinetic movements, highlighting a prominent role of SChIs in modulating basal ganglia network dynamics. We note that a recent study reported a lack of movement changes upon optogenetic simulation of SChIs in virally labeled animals (32). It is possible that sufficient activation of SChIs is needed to produce an observable behavioral effect, and our experimental conditions using transgenic mice may allow us to activate sufficient numbers of SChIs to bias behavior.

Interestingly, we observed unexpected changes in rotational behavior in both directions after unilateral SChI stimulation. It is possible that unilateral stimulation of SChIs could engage not only the ipsilateral CBT loop but also the contralateral CBT loop through M1 bilaterally projecting intratelencephalic neurons (36). Alternatively, because both ACh and glutamate are released from SChIs (37) and can potentially activate both D1 and D2 populations of MSNs, it is also possible that the direction of rotation depends on the relative excitation level of these two populations.

Although the source of the exaggerated beta oscillations in PD has not yet been established, we suggest here that it may consist of multiple, interacting sources. At least two independent beta generators are suggested by the distinct time course of coherence between deep layers of M1 and the striatum upon SChI activation, with coherence at higher beta frequencies of ∼22–30 Hz increasing and then rapidly dissipating, and coherence at lower beta frequencies of ∼15–22 Hz staying elevated throughout SChI activation. The dissipating coherence in the high beta frequency range despite consistently elevated beta power suggests at least two independent sources of high frequency beta, possibly one from basal ganglia networks and another in M1. An independent beta generator in M1 is consistent with in vitro work, demonstrating that deep layers of M1 can generate high frequency beta oscillations (∼27 Hz) in layer V in the presence of carbachol and kainate (38). Additionally, we observed decreased coherence

between striatum and superficial M1 throughout the entire beta frequency range (15–30 Hz) despite significant increases in beta power in these structures upon SChI stimulation, suggesting an additional source of beta oscillations within the CBT loop. It has been observed that both high and low frequency beta oscillations are elevated in the basal ganglia in parkinsonian states and are correlated with different PD motor symptoms (39). The observed dissociation of different frequency beta oscillations here, in normal mice with elevated striatal cholinergic tone, may indicate possible distinct network sources that generate PD-related beta-band oscillations.

Whereas the literature proposes several putative mechanisms of CBT loop beta oscillation generation, our previous work suggests that networks of striatal MSNs can produce beta oscillations with sufficient MSN excitation (23). Because muscarinic receptors can increase MSN excitability by decreasing the M-current, our computational model predicts that muscarinic receptor blockade will interfere with the beta-producing mechanism in the striatum. This mechanism is supported by the experimental results of the present study demonstrating that striatal muscarinic blockade significantly decreases SChI stimulation-induced beta oscillations in the striatum. If the beta-producing mechanism of high striatal cholinergic tone plays a role in PD, our work suggests that modalities reducing striatal cholinergic tone may be instrumental in alleviating excessive beta oscillations in the parkinsonian CBT loop, along with their correlated motor symptoms. In fact, systemic antimuscarinic drugs were the sole pharmacologic treatment for PD until the late 1960s, when L-dopa was introduced (40), although their clinical use is limited by neuropsychiatric and cognitive side effects (41).

The literature proposes two other origins of pathologic beta oscillations in PD: the subthalamic nucleus (STN)-globus pallidus externa (GPe) circuit (42) and M1 (38). The former hypothesis depends on the presence of plastic changes attributable to chronic loss of dopamine in the STN-GPe network. Such mechanisms may be applicable to the parkinsonian state. However, our results suggest that neither chronic plastic changes nor chronic low dopamine is needed to produce robust beta oscillations within the CBT loop upon SChI stimulation. We note that a similar finding is evident in M1, where robust beta oscillations can emerge in nonparkinsonian M1 slices in the presence of sufficient excitation with carbachol and kainate (38, 43). Excitation of M1 neurons occurs in response to increased D1 MSN spiking and can also occur transiently to a subset of M1 neurons in response to D2 MSN spiking (44). To what extent M1 generated beta oscillations are induced under the conditions of SChI stimulation is an interesting topic of future study. Excitation to M1 during SChI stimulation may depend on the amount and timing of excitation provided to D1 versus D2 MSNs (44).

Recent studies (45, 46) showed that microinfusions of GABAergic antagonists in GPe failed to reduce beta oscillatory activities at the site of infusion in 1-methyl-4-phenyl-1,2,3,6-tetrahydropyridine (MPTP) neurotoxin-induced Parkinsonian monkeys, although infusion of glutamatergic antagonists in GPe and STN reduced beta oscillations. These results are consistent with the view that the striatum is a source of beta oscillations, whereas the STN-GPe network serves as an amplifier of the striatally generated oscillations. In our framework, mechanisms that decrease the activity of STN or GPe will compromise the beta amplification mechanism and, thus, decrease beta oscillations. Correspondingly, mechanisms that increase the connectivity of STN and GPe (e.g., suppression of GPe lateral inhibition with GABAergic antagonist) may increase beta oscillations. This observation, taken together with the fact that microinfusion of GABAergic antagonists blocks a small amount of striatal inputs to GPe, suggests that substantial change to GPe beta oscillatory activity would not be expected with the microinfusion experiments performed in refs. 45 and 46.

Although much of the oscillatory spectrum in striatum is elevated during SChI stimulation, these elevations do not occur across the entire frequency range and, thus, are not considered a broadband increase in power. In contrast, scopolamine infusion decreased power at all frequencies, as expected with a broadband decrease (Fig. 5*A*). However, in the presence of scopolamine, SChIs remained as effective as in the absence of scopolomine in elevating high gamma oscillations, but not beta or low gamma, suggesting a mechanistic separation between the generators of these frequencies. Additionally, coherence between striatum and the deep layers of M1 increased for beta and low gamma, but not high gamma, despite increases in power in both structures in all these frequency bands. Thus, beta and low gamma elevations appear to be both selectively elevated and coordinated in the CBT circuit during SChI stimulation, whereas high gamma may represent increased neuronal excitability (26).

SChI activation also produced electrophysiological effects that are not commonly observed in PD, including gamma power (30–100 Hz) elevation in cortex and striatum. Finely tuned gamma oscillations in the range of 60–90 Hz are a consistent feature of basal ganglia and thalamic recordings (47) that are diminished in PD patients in the absence of dopaminergic replacement (17, 18). However, rather than an increase in finely tuned gamma, here we observed a broader-band gamma power increase, which may represent a general increase in neuronal activity (26). Laser-induced striatal high gamma oscillations remained elevated after either muscarinic or nicotinic blockade, suggesting that ACh is not involved in the generation of striatal high gamma oscillations. Glutamate, which is also coreleased from SChIs, may be responsible for the increase in high gamma oscillations during SChI stimulation (37). Striatal low gamma oscillations, however, are more correlated with beta in our current study, consistent with that observed in the basal ganglia of rats (10). While it is unclear how low gamma is generated in the CBT circuits, evidence from the ventral striatum of rats have suggested that low and high gamma have distinct sources, with dopaminergic drugs selectively diminishing the power of low gamma and enhancing the power of high gamma (48). In addition, low and high gamma oscillations are increased at different times during a spatial decision task (49), likely coordinated by different sets of FS interneurons (48, 49). Further work is required to delineate the mechanisms that result in increased M1 low and high gamma oscillatory activity due to increased striatal cholinergic tone.

Interneurons represent a small proportion of striatum, but these neurons can strongly modulate striatal output. The proportion of interneurons in striatum is 4–5% in mouse, >23% in monkey (50), and up to at least 25% in human (50), suggesting a more prominent role for striatal interneurons in nonhuman primates and humans. The majority of GABAergic interneurons in the striatum are parvalbumin-positive FS interneurons, which project primarily to the MSNs. Although FS interneurons are excited by nicotinic agonists (51), optogenetic activation of SChIs failed to increase FS interneuron spiking in one study (52). Additionally, optogenetic stimulation of SChIs in ChAT-ChR2 mice elicits both fast and slow inhibitory postsynaptic potentials in MSNs by nicotinic-mediated GABA release from dopamine projections to striatum (53) and neuropeptide Y-expressing neurogliaform GABAergic interneurons, resulting in inhibition of MSNs (52). However, nicotinic receptors generally quickly desensitize and, thus, we did not expect GABAergic blockade of MSN spiking to continue through the 5 s of stimulation used in our current study. Accordingly, our study reveals that nicotinic receptor blockade by mecamylamine did not change the spectral profile of either beta or gamma oscillations in the striatum or cortex over 5-s periods. This result suggests that SChI-induced GABA release does not exert long-term control over the SChI-induced oscillations along the corticostriatal circuit.

In contrast, we show that SChI-induced elevation of beta and low gamma oscillations depends on muscarinic receptors, because striatal scopolamine infusion lowered SChI-induced spectral power elevations of these oscillations. ACh acts through muscarinic receptors present on MSNs to decrease the activity of KCNQ (M-current) and Kir2.3 channels, thereby increasing MSN excitability (54, 55). In addition, ACh also works through muscarinic receptors to inhibit the release of glutamate from corticostriatal terminals and GABA from striatal FS cells (51, 56). Thus, muscarinic receptor activity diminishes the impact of glutamatergic and GABAergic input on MSNs while simultaneously increasing the excitability of MSNs. Therefore, muscarinic receptor activation could potentially accentuate the intrinsic dynamics of the MSN network.

It is surprising that stimulation of a single interneuron type, SChIs, can reversibly reproduce some of the key electrophysiological and behavioral manifestations of PD in normal mice, including increased beta oscillations in corticostriatal circuits, increased coherence between the cortex and the basal ganglia, and decreased mobility. SChI stimulation also increased rotational behavior, a phenotype often observed in mice rendered parkinsonian by a 6-OHDA lesion (57). These results suggest that the exaggerated beta oscillations in PD may reflect an uncontrolled expression of a normal dynamical state of the CBT network, a state that is directly modulated by SChI excitability.

In summary, we provide evidence supporting the existence of a beta frequency pacemaker within the CBT loop that can be activated by stimulation of striatal cholinergic interneurons via striatal muscarinic receptors. Combined with our findings of behavioral deficits similar to those in PD upon stimulating this pacemaker, our results suggest that the beta oscillations in PD may be an overexpression of normal CBT network dynamics due to a striatal dopamine/ACh imbalance, rather than a de novo oscillation due to a PD-induced network pathology.

ACKNOWLEDGMENTS. We thank Kimberley H. Ching for assistance with immunocytochemistry and illustration of recording configuration, Moona Abdulkerim for assistance with behavioral experiments, members of the X.H. laboratory and N.K. laboratory for various technical support and suggestions over the course of the study, and our reviewers for their helpful comments and suggestions. X.H. acknowledges funding from NIH Director's New Innovator Award 1DP2NS082126, NINDS Grant 1R21NS078660, Pew Foundation, Alfred P. Sloan Foundation, Boston University Biomedical Engineering Department, and Boston University Photonic Center. X.H. and M.M.M acknowledge CRCNS NIH Grant 1R01NS081716, and N.K. acknowledges NSF DMS-1042134-5.

1. Brown P (2007) Abnormal oscillatory synchronisation in the motor system leads to impaired movement. *Curr Opin Neurobiol* 17(6):656–664.
2. Little S, Pogosyan A, Kuhn AA, Brown P (2012) β band stability over time correlates with Parkinsonian rigidity and bradykinesia. *Exp Neurol* 236(2):383–388.
3. Brown P, Williams D (2005) Basal ganglia local field potential activity: Character and functional significance in the human. *Clinical Neurophysiol* 116(11):2510–2519.
4. Kühn AA, Kupsch A, Schneider GH, Brown P (2006) Reduction in subthalamic 8-35 Hz oscillatory activity correlates with clinical improvement in Parkinson's disease. *Eur J Neurosci* 23(7):1956–1960.
5. Kühn AA, et al. (2008) High-frequency stimulation of the subthalamic nucleus suppresses oscillatory beta activity in patients with Parkinson's disease in parallel with improvement in motor performance. *J Neurosci* 28(24):6165–6173.
6. Herrojo Ruiz M, Brücke C, Nikulin VV, Schneider GH, Kühn AA (2014) Beta-band amplitude oscillations in the human internal globus pallidus support the encoding of sequence boundaries during initial sensorimotor sequence learning. *Neuroimage* 85(Pt 2):779–793.
7. Sochurkova D, Rektor I (2003) Event-related desynchronization/synchronization in the putamen. An SEEG case study. *Exp Brain Res* 149(3):401–404.
8. Bartolo R, Merchant H (2015) β oscillations are linked to the initiation of sensory-cued movement sequences and the internal guidance of regular tapping in the monkey. *J Neurosci* 35(11):4635–4640.
9. Courtemanche R, Fujii N, Graybiel AM (2003) Synchronous, focally modulated beta-band oscillations characterize local field potential activity in the striatum of awake behaving monkeys. *J Neurosci* 23(37):11741–11752.
10. Leventhal DK, et al. (2012) Basal ganglia beta oscillations accompany cue utilization. *Neuron* 73(3):523–536.
11. Berke JD, Okatan M, Skurski J, Eichenbaum HB (2004) Oscillatory entrainment of striatal neurons in freely moving rats. *Neuron* 43(6):883–896.
12. Feingold J, Gibson DJ, DePasquale B, Graybiel AM (2015) Bursts of beta oscillation differentiate postperformance activity in the striatum and motor cortex of monkeys performing movement tasks. *Proc Natl Acad Sci USA* 112(44):13687–13692.
13. Schmidt R, Leventhal DK, Mallet N, Chen F, Berke JD (2013) Canceling actions involves a race between basal ganglia pathways. *Nat Neurosci* 16(8):1118–1124.
14. Sharott A, et al. (2005) Dopamine depletion increases the power and coherence of beta-oscillations in the cerebral cortex and subthalamic nucleus of the awake rat. *Eur J Neurosci* 21(5):1413–1422.
15. Mallet N, et al. (2008) Disrupted dopamine transmission and the emergence of exaggerated beta oscillations in subthalamic nucleus and cerebral cortex. *J Neurosci* 28(18):4795–4806.
16. Costa RM, et al. (2006) Rapid alterations in corticostriatal ensemble coordination during acute dopamine-dependent motor dysfunction. *Neuron* 52(2):359–369.
17. Brown P, et al. (2001) Dopamine dependency of oscillations between subthalamic nucleus and pallidum in Parkinson's disease. *J Neurosci* 21(3):1033–1038.
18. Kempf F, et al. (2009) Gamma activity and reactivity in human thalamic local field potentials. *Eur J Neurosci* 29(5):943–953.
19. Gerfen CR, Surmeier DJ (2011) Modulation of striatal projection systems by dopamine. *Annu Rev Neurosci* 34:441–466.
20. DeBoer P, Heeringa MJ, Abercrombie ED (1996) Spontaneous release of acetylcholine in striatum is preferentially regulated by inhibitory dopamine D2 receptors. *Eur J Pharmacol* 317(2–3):257–262.
21. Ikarashi Y, Takahashi A, Ishimaru H, Arai T, Maruyama Y (1997) Regulation of dopamine D1 and D2 receptors on striatal acetylcholine release in rats. *Brain Res Bull* 43(1):107–115.
22. Ding J, et al. (2006) RGS4-dependent attenuation of M4 autoreceptor function in striatal cholinergic interneurons following dopamine depletion. *Nat Neurosci* 9(6):832–842.
23. McCarthy MM, et al. (2011) Striatal origin of the pathologic beta oscillations in Parkinson's disease. *Proc Natl Acad Sci USA* 108(28):11620–11625.
24. Pisani A, Bernardi G, Ding J, Surmeier DJ (2007) Re-emergence of striatal cholinergic interneurons in movement disorders. *Trends Neurosci* 30(10):545–553.
25. Han X, et al. (2009) Millisecond-timescale optical control of neural dynamics in the nonhuman primate brain. *Neuron* 62(2):191–198.
26. Manning JR, Jacobs J, Fried I, Kahana MJ (2009) Broadband shifts in local field potential power spectra are correlated with single-neuron spiking in humans. *J Neurosci* 29(43):13613–13620.
27. Ramanathan S, Hanley JJ, Deniau JM, Bolam JP (2002) Synaptic convergence of motor and somatosensory cortical afferents onto GABAergic interneurons in the rat striatum. *J Neurosci* 22(18):8158–8169.
28. Kühn AA, et al. (2009) Pathological synchronisation in the subthalamic nucleus of patients with Parkinson's disease relates to both bradykinesia and rigidity. *Exp Neurol* 215(2):380–387.
29. Stein E, Bar-Gad I (2013) β oscillations in the cortico-basal ganglia loop during parkinsonism. *Exp Neurol* 245:52–59.
30. Pollok B, et al. (2012) Motor-cortical oscillations in early stages of Parkinson's disease. *J Physiol* 590(13):3203–3212.
31. Devergnas A, Pittard D, Bliwise D, Wichmann T (2014) Relationship between oscillatory activity in the cortico-basal ganglia network and parkinsonism in MPTP-treated monkeys. *Neurobiol Dis* 68:156–166.
32. Maurice N, et al. (2015) Striatal cholinergic interneurons control motor behavior and basal ganglia function in experimental parkinsonism. *Cell Reports* 13(4):657–666.
33. Gittis AH, et al. (2011) Selective inhibition of striatal fast-spiking interneurons causes dyskinesias. *J Neurosci* 31(44):15727–15731.
34. Kravitz AV, et al. (2010) Regulation of parkinsonian motor behaviours by optogenetic control of basal ganglia circuitry. *Nature* 466(7306):622–626.
35. Wang Z, Rebec GV (1993) Neuronal and behavioral correlates of intrastriatal infusions of amphetamine in freely moving rats. *Brain Res* 627(1):79–88.
36. Shepherd GM (2013) Corticostriatal connectivity and its role in disease. *Nat Rev Neurosci* 14(4):278–291.
37. Higley MJ, et al. (2011) Cholinergic interneurons mediate fast VGluT3-dependent glutamatergic transmission in the striatum. *PLoS One* 6(4):e19155.
38. Yamawaki N, Stanford IM, Hall SD, Woodhall GL (2008) Pharmacologically induced and stimulus evoked rhythmic neuronal oscillatory activity in the primary motor cortex in vitro. *Neuroscience* 151(2):386–395.
39. Toledo JB, et al. (2014) High beta activity in the subthalamic nucleus and freezing of gait in Parkinson's disease. *Neurobiol Dis* 64:60–65.
40. Fox SH (2013) Non-dopaminergic treatments for motor control in Parkinson's disease. *Drugs* 73(13):1405–1415.
41. Katzenschlager R, Sampaio C, Costa J, Lees A (2003) Anticholinergics for symptomatic management of Parkinson's disease. *Cochrane Database Syst Rev* (2):CD003735.
42. Holgado AJ, Terry JR, Bogacz R (2010) Conditions for the generation of beta oscillations in the subthalamic nucleus-globus pallidus network. *J Neurosci* 30(37):12340–12352.
43. Lacey MG, et al. (2014) Spike firing and IPSPs in layer V pyramidal neurons during beta oscillations in rat primary motor cortex (M1) in vitro. *PLoS One* 9(1):e85109.
44. Oldenburg IA, Sabatini BL (2015) Antagonistic but not symmetric regulation of primary motor cortex by basal ganglia direct and indirect pathways. *Neuron* 86(5):1174–1181.
45. Bar-Gad I, Elias S, Vaadia E, Bergman H (2004) Complex locking rather than complete cessation of neuronal activity in the globus pallidus of a 1-methyl-4-phenyl-1,2,3,6-

tetrahydropyridine-treated primate in response to pallidal microstimulation. *J Neurosci* 24(33):7410–7419.
46. Tachibana Y, Iwamuro H, Kita H, Takada M, Nambu A (2011) Subthalamo-pallidal interactions underlying parkinsonian neuronal oscillations in the primate basal ganglia. *Eur J Neurosci* 34(9):1470–1484.
47. Jenkinson N, Kühn AA, Brown P (2013) γ oscillations in the human basal ganglia. *Exp Neurol* 245:72–76.
48. Berke JD (2009) Fast oscillations in cortical-striatal networks switch frequency following rewarding events and stimulant drugs. *Eur J Neurosci* 30(5):848–859.
49. van der Meer MA, Redish AD (2009) Low and high gamma oscillations in rat ventral striatum have distinct relationships to behavior, reward, and spiking activity on a learned spatial decision task. *Front Integr Nuerosci* 3:9.
50. Graveland GA, Williams RS, DiFiglia M (1985) A Golgi study of the human neostriatum: Neurons and afferent fibers. *J Comp Neurol* 234(3):317–333.
51. Koós T, Tepper JM (2002) Dual cholinergic control of fast-spiking interneurons in the neostriatum. *J Neurosci* 22(2):529–535.
52. English DF, et al. (2011) GABAergic circuits mediate the reinforcement-related signals of striatal cholinergic interneurons. *Nat Neurosci* 15(1):123–130.
53. Nelson AB, et al. (2014) Striatal cholinergic interneurons Drive GABA release from dopamine terminals. *Neuron* 82(1):63–70.
54. Shen W, Hamilton SE, Nathanson NM, Surmeier DJ (2005) Cholinergic suppression of KCNQ channel currents enhances excitability of striatal medium spiny neurons. *J Neurosci* 25(32):7449–7458.
55. Shen W, et al. (2007) Cholinergic modulation of Kir2 channels selectively elevates dendritic excitability in striatopallidal neurons. *Nat Neurosci* 10(11):1458–1466.
56. Higley MJ, Soler-Llavina GJ, Sabatini BL (2009) Cholinergic modulation of multivesicular release regulates striatal synaptic potency and integration. *Nat Neurosci* 12(9):1121–1128.
57. Deumens R, Blokland A, Prickaerts J (2002) Modeling Parkinson's disease in rats: An evaluation of 6-OHDA lesions of the nigrostriatal pathway. *Exp Neurol* 175(2): 303–317.
58. Madisen L, et al. (2012) A toolbox of Cre-dependent optogenetic transgenic mice for light-induced activation and silencing. *Nat Neurosci* 15(5):793–802.
59. Bokil H, Andrews P, Kulkarni JE, Mehta S, Mitra PP (2010) Chronux: A platform for analyzing neural signals. *J Neurosci Methods* 192(1):146–151.